# Utilization of air granulated basic oxygen furnace slag as a binder in belite calcium sulfoaluminate cement: A sustainable alternative

Journal of Cleaner Production 436 (2024) 140539

Contents lists available at ScienceDirect

Journal of Cleaner Production

journal homepage: www.elsevier.com/locate/jclepro

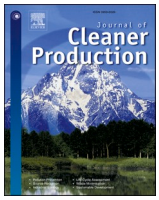

# Utilization of air granulated basic oxygen furnace slag as a binder in belite calcium sulfoaluminate cement: A sustainable alternative

Muhammad Jawad Ahmed [a,*], Sterenn Durand [b], Marc Antoun [a], Florent Gauvin [a], Sofiane Amziane [b], H.J.H. Brouwers [a]

[a] Department of Built Environment, Eindhoven University of Technology, Eindhoven, the Netherlands
[b] Universitè Clermont Auvergne, CNRS, SIGMA Clermont, Institute Pascal, Clermont-Ferrand, France

ARTICLE INFO

Handling editor: Panos Seferlis

*Keywords:*
Reactivity
Hydration products
BCSA cement
Microstructure
Supplementary cementitious materials

ABSTRACT

Basic oxygen furnace (BOF) slag negatively impacts ordinary Portland cement performance when replacement levels exceed 5%. This necessitates the exploration of alternative applications for the slag. Simultaneously, a high-volume slag utilization is desired to benefit slag recycling as supplementary cementitious materials. Therefore, this study aims to optimize the air granulated BOF slag substitution potential in belite calcium sulfoaluminate cement by investigating the hydration products in standard mortar. The reactivity of the novel binder is correlated with workability, and mechanical performance by thermal, mineralogical, and microstructure analysis. Consequently, the 10–30% replacement delays the final setting time by inhibiting the ettringite formation leading to a decrease in mechanical performance till 28 days. At later ages (28–180 days), the 30–50% substitution exhibited the synergy in mechanical performance, which is attributed to the hydrogarnet, calcium silicate hydrate, and strätlingite formation. Moreover, all the mortar samples exhibited heavy metals' leaching and drying shrinkage below the permissible limit.

## 1. Introduction

Environmental challenges, such as climate change and resource depletion have put a spotlight on the need for a low-carbon (Benhelal et al., 2013), resource-efficient (Shen and Forssberg, 2003), and closed-loop economy for sustainable development (Shen et al., 2015). The main challenge lies in the utilization of industrial residues to get zero-waste flow sheets (Link et al., 2015). The cement industry is facing the same challenges of sustainable solutions due to increasing global demand and is expected to reach 12–23% by 2050 (Favier et al., 2018). The efficient use of alternative materials for fuels and clinkers is the main strategy to reduce $CO_2$ emissions (Schneider et al., 2011). One of the solutions is belite calcium sulfoaluminate types of cement (BCSA) due to a reduction in $CO_2$ emission by 30% than conventional Portland cement. BCSA requires a lower kiln firing temperature of ~1250 °C leading to a lesser amount of $NO_x$ emissions and better grindability as compared to Portland cement clinker. However, the limited availability of raw materials as well as low demand for these types of cement makes the product expensive and can only be utilized for special applications. Moreover, efforts are required to control appropriate mix design, for instance, 1) early hydration kinetics and volume stability due to the amount of calcium sulfate (Chen et al., 2022), 2) the early setting needs to be controlled with admixtures (Hargis et al., 2017), 3) the effect of altering these parameters on the later age concrete performance and durability (Ludwig and Zhang, 2015; Telesca et al., 2020). Therefore, a significant amount of industrial side streams such as blast furnace slag, silica fumes, waste glass, fly ash, etc. have been added alongside calcium sulfoaluminate cement in concrete to study the more efficient use of the building materials (Chi et al., 2021; Iacobescu et al., 2013).

Basic oxygen furnace (BOF) slag is the tremendously available byproduct of steel-making process generating 90–150 kg of the slag for every tonne of crude steel (Guo et al., 2018). In Europe, approximately 10 Mt/year of BOF slag is produced, and approximately 23% directly stacked piles occupy the land resources (Horii et al., 2013). The recycling of BOF slag gained much attention in terms of supplementary cementitious materials (SCMs) in building materials. Because the first choice of SCMs such as granulated blast furnace slag (GBFS) and fly ashes (FA) sources of adequate quality are limited in Europe and

* Corresponding author.
*E-mail addresses:* m.ahmed@tue.nl (M.J. Ahmed), duransterenn@gmail.com (S. Durand), m.antoun@tue.nl (M. Antoun), F.Gauvin@tue.nl (F. Gauvin), sofiane.amziane@uca.fr (S. Amziane), jos.brouwers@tue.nl (H.J.H. Brouwers).

https://doi.org/10.1016/j.jclepro.2023.140539
Received 10 August 2023; Received in revised form 2 December 2023; Accepted 30 December 2023
Available online 2 January 2024

unlikely to increase (Scrivener et al., 2018). Applying BOF slag as cementitious material will not only diminish the landfilled/land occupation but also reduce the need for natural resources. The recycling and reuse of slag have many challenges such as low hydraulic activity, leaching of heavy metals (Cr and V) (De Windt et al., 2011), inhibition of cementitious reaction (Jiang et al., 2018), and poor grindability, etc. seriously restricts its application as supplementary cementitious material (SCM) in OPC (Zhuang and Wang, 2021).

Several Strategies have been reported to address the recycling challenges of the slag through activation such as chemical activation (Kaja et al., 2021), mineral modification (Tsakiridis et al., 2008), weathering (Li and Dai, 2018), carbonation, and high-temperature curing (Eloneva, 2010). But no profound economic application has been reported yet. One way to improve slag reactivity is to enhance the cooling speed by air granulation (Schollbach et al., 2021). Air granulation is reported to be more sustainable in terms of heat recovery when the slag tapping temperature lies between 1250 and 1700 °C (Engström et al., 2010). Our study showed (Jawad Ahmed et al., 2023) that the air granulation of BOF slag did not improve the reactivity significantly except for the grindability. Moreover, a low percentage merely up to 5% by volume can be replaced as a binder in OPC (Jawad Ahmed et al., 2023; Wulfert et al., 2017) which demands alternative building products. An efficient building product is desired in which slag can be recycled in a high volume as SCM.

In this regard, a few studies have reported that the steel slag addition in calcium sulfoaluminate cement (CSA) as SCM brings many benefits of improved workability and performance (Liao et al., 2020; Martins et al., 2022; Xue et al., 2016). However, the strength loss of CSA-based cement is reported at later ages which is attributed to the ettringite decomposition (Hargis et al., 2014). The BOF slag is a good source of belite and ferrite phases which can be used alongside "Belite-Ye'elimite-Ferrite" (BYF) clinker. BYF clinkers (e.g., "Aether" or "Ternocem") have the potential to replace Portland cement clinker as well as Portland-slag cement in many applications. The BOF slag contains dicalcium silicate and brownmillerite as main hydration phases which would enrich the hydration matrix with calcium silicate hydrate, ettringite, hydrotalcite, etc. (Santos et al., 2023). Furthermore, these newly formed hydration products would provide later-age stability besides enhancing the immobilization potential of heavy metals (Peysson et al., 2005). The role of BOF slag as a binder is well understood in OPC but the effect of BOF slag on the BCSA cement hydration, workability, mechanical performance, shrinkage as well as environmental risks requires a systematic understanding (Zhuang and Wang, 2021). To the author's best knowledge, there is no information available for the BCSA- (air granulated) BOF slag-based novel binder. Therefore, this study aims to understand the effect of air granulated BOF slag substitution in BCSA cement. For this purpose, the replacement of 10, 20, 30, 40, and 50% BCSA cement by the slag in mortars is chosen to optimize the substitutional potential. The effect of the BCSA-slag cluster's reactivity on workability, mechanical performance, and drying shrinkage over time is studied through thermal, mineralogical, and microstructural analysis to understand the novel binder application. Moreover, the potential leaching of heavy metals especially V and Cr is evaluated by ICP-OES to assess the environmental risk.

## 2. Materials and methods

### 2.1. Materials preparation and characterization

Air granulated BOF slag taken from regular production at Tata Steel Europe in Ijmuiden. The air granulation process of BOF slag has been studied elsewhere in detail (Schollbach et al., 2021). The 1–4 mm fraction that accounts for ~90% of total air granulation yield is milled and used for the study. Belite calcium sulfoaluminate cement (BCSA) cement is supplied by Vicat cement.

A representative slag sample was chosen by using a static sample splitter. The air granulated BOF slag was dried in an oven at 100 °C to remove possible moisture. The slag was ground for 30 min at 912 rpm to get fine particles via disk mill (Retsch RS 300 XL). To ensure the consistency of the feed, a 1 kg weighed amount is placed in the disk mill. The PSD (particle size distribution) was determined using Mastersizer2000 from Malvern and the milled sample was dispersed in isopropanol as a solvent so as not to trigger the hydration reaction. To understand the impact of specific surface area (SSA) on the hydration kinetics, the nitrogen adsorption (Tristar II 3020 V1.03 series micrometer) at 77K was measured using BET (Brunauer-Emmett-Teller) methods. A minimum of 0.5 g sample is used to have representative measurement, and the powder sample is degassed under vacuum at high temperature. The specific density of the milled BOF slag was measured by a Helium pycnometer (AccuPys II 1340). During each test, 10 measurements are recorded, and the density is an average of these values. The PSD and SSA are presented in Fig. 1 (a).

Before XRF analysis, mass change was measured by heating slag samples at 1000 °C for 2h. For the preparation of fused beads, the residue from the LOI was mixed with borate flux by keeping the sample to flux ratio (1:12) respectively, a mixture of 67% $Li_2BO_7$ and 33% $LiBO_2$ (Claisse). Moreover, 150 μL of 4 M LiBr was added to the mix as a non-wetting agent. The mixture was placed in a borate fluxer oven (classisse leNeo) for 24 min at 1065 °C. The chemical oxide composition of the raw material was determined with X-ray fluorescence (XRF; PANalytical Epsilon 3, standardless) using fused beads as shown in Table 1. The air granulated BOF slag exhibited negative loss of ignition (mass gain) due to the conversion of ferrous oxide into ferric oxide and contained a high amount of $Fe_2O_3$ (~27 wt%). The BCSA cement contains a higher amount of $Al_2O_3$ (~15.3 wt%) as compared to the slag which is considered to be an important elemental oxide for the mineral modifier to improve the reactivity of the BOF slag (Liu et al., 2019).

X-ray powder diffractograms (XRD) were acquired using a Bruker D4 diffractometer with X-ray Co radiation X-ray source (Detector: LynxEye). The instrument has a fixed/variable divergence slit with an opening of 0.5° and 0.04 rad Soller slits. Reflections were measured between 5° and 90° 2 Theta (θ) with a step size of 0.02°. The 1–90 days cured sample at room temperature was crushed, and hydration was stopped via solvent (Isopropanol, Diethyl ether) exchange method. All samples for qualitative analysis were prepared via back-loading. The synthesized phases were identified with X'Pert Highscore Plus 2.2 employing the ICDD PDF-2 database. The diffractogram of the raw material is shown in Fig. 1 (b). The BCSA contains mineral phases ye'elimite, larnite/belite, α′-dicalcium silicate ($C_2S$), anhydrite, tricalcium aluminate, brownmillerite, calcite with traces of Mg and Fe-wüstite phases. The air granulated BOF slag exhibited a high amount of α′-$C_2S$ (high-temperature modification) alongside larnite, brownmillerite, perovskite, and Mg, Fe-wüstite with traces of calcite. The BCSA cement contains a significant amount of ye'elimite alongside anhydrite and tricalcium aluminate which is responsible for early-age reactivity leading to high early strength. While the air granulated BOF slag contains a high amount of the $C_2S$ (α′-modification, larnite) and brownmillerite that would contribute to the later age strength of the BSCA-slag clusters (Chen et al., 2022; Schollbach et al., 2021).

### 2.2. Mortar study

#### 2.2.1. Mix design

The mortar mix design was adopted according to EN 196-1 standard with an effective water-to-binder ratio (w/b) of 0.5. The density of BCSA and air granulated BOF slag are 2.8 and 3.5 g/cm$^3$ respectively.

The mortar sample is composed of 25% binder and 75% standard sand by volume as shown in Table 2. The 100% BCSA sample was chosen as a reference and replacements by volume of 10, 20, 30, 40, and 50% BOF slag were made to optimize the effective substitution in BCSA. The fresh sample was cast in plastic molds of 160 × 40 × 40 mm covered with a thin plastic film for 24 h, then de-molded and cured at room

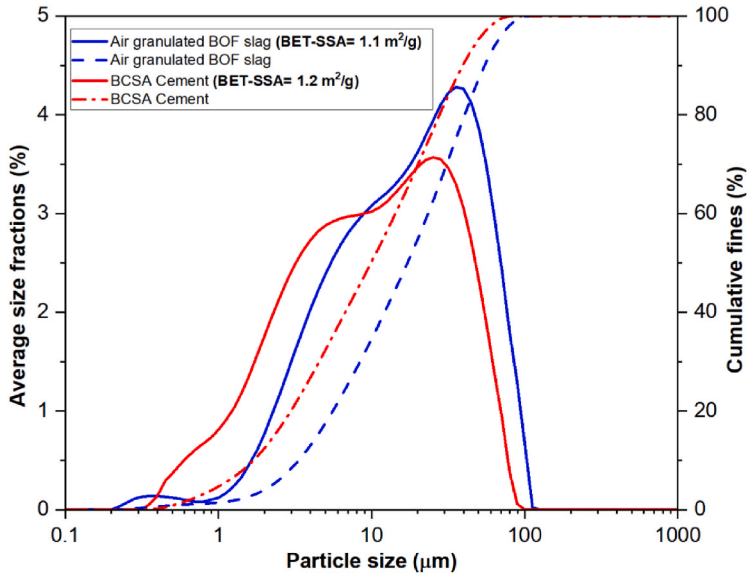


(a)

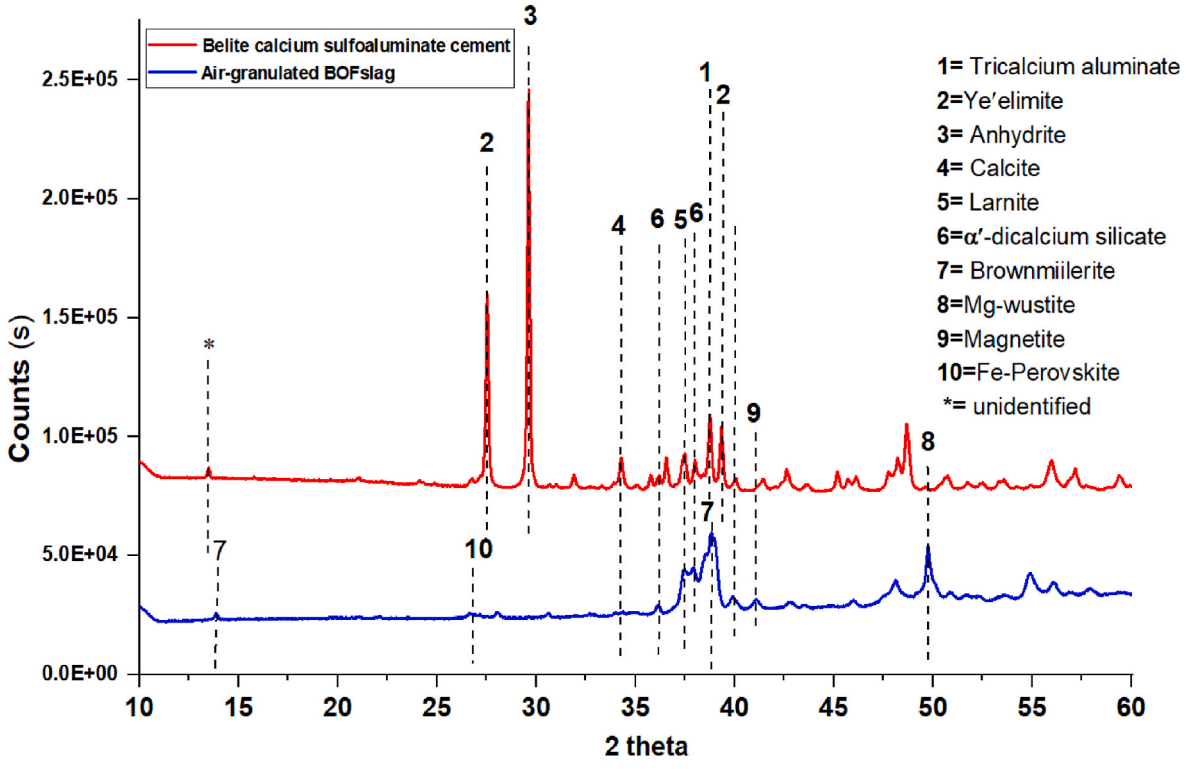


(b)

**Fig. 1.** a) The PSD (particle size distribution) of the raw material. In the inset, specific surface area (SSA) is obtained via the BET method. b) X-ray diffraction pattern of BCSA and air granulated BOF slag with labeled peaks.

temperature until their testing age.

### 2.2.2. *Fresh properties*

The flow table was performed to measure the flowability of fresh paste according to EN 1015–3:2004. The w/b ratio was kept constant, and flow was adjusted with a superplasticizer (Sika ViscoFlow®-37 con. 32% SP-Polycarboxylate ether). This test consists of filling a truncated cone with our paste, then removing the mold in 3 s, and subjecting the cone to 15 shocks. Finally, we measured the average of 3 diameters. The setting time is measured according to NF EN 196-3 with a Vicat needle.

**Table 1**
Oxide composition of air granulated BOF slag and BCSA cement.

| Material | MgO | $Al_2O_3$ | $SiO_2$ | $SO_3$ | $P_2O_5$ | CaO | $TiO_2$ | $V_2O_5$ | $Cr_2O_3$ | MnO | $Fe_2O_3$ | LOI |
|---|---|---|---|---|---|---|---|---|---|---|---|---|
| **BCSA Cement** (wt.%) | 0.7 | 15.3 | 8.0 | 13.5 | – | 50.6 | 1.1 | – | 0.1 | 0.1 | 10.6 | 4.04 |
| **Air-granulated BOF slag** (wt.%) | 7.3 | 1.3 | 12.5 | – | 1.2 | 44.6 | 1.3 | 0.7 | 0.3 | 3.9 | 26.8 | −0.02 |

LOI = loss on ignition.

**Table 2**
Mix design proportions of the BCSA-slag mortars (vol. %).

| MIX ID | BCSA Cement | Air granulated BOF slag | Standard Sand | water/binder | BCSA Replacement (%) | Superplasticizer (% of total binder) |
|---|---|---|---|---|---|---|
| REF | 0.25 | 0 | 0.75 | 0.5 | 0 | 0.24 |
| 10% BOF | 0.22 | 0.03 | 0.75 | 0.5 | 10 | 0.19 |
| 20% BOF | 0.2 | 0.06 | 0.74 | 0.5 | 20 | 0.17 |
| 30% BOF | 0.17 | 0.09 | 0.74 | 0.5 | 30 | 0.14 |
| 40% BOF | 0.15 | 0.12 | 0.73 | 0.5 | 40 | 0.10 |
| 50% BOF | 0.12 | 0.15 | 0.73 | 0.5 | 50 | 0.00 |

The test consists of measuring the time that a Vicat needle (S = 1 $mm^2$, mass = 300 g) does not sink to the bottom of a pellet of pure cement of standardized consistency.

#### 2.2.3. Drying shrinkage and mass loss

The drying shrinkage and the drying mass loss were measured according to DIN 52,450 to determine the long-term stability. For this purpose, the specimens were cured in an acclimatized room at 21 ± 2 °C and relative humidity of 60 ± 5% RH, where the measurement was carried out for 72 days till a further change in values became constant.

#### 2.2.4. Mechanical properties

The compressive and flexural strength of the mortar specimens were evaluated after 1, 3, 7, 28, 90, and 180 days. After casting, the specimen surface was covered with a thin film to prevent water evaporation besides carbonation and placed for curing under standard conditions (21 ± 3 °C, 95 ± 3% relative humidity). The compressive, as well as flexural strength, were measured at a speed of 2400 and 50 N/s respectively. The average of three specimens was calculated to evaluate the reproducibility of results.

#### 2.2.5. Thermal analysis

Early age hydration of raw materials, as well as BCSA-slag paste having 0.5 w/b ratios, was analyzed with a TAM Air isothermal instrument at 20 °C for 7 days.

Thermal gravimetric (TG) analysis was performed on the cured sample via Jupiter STA 449 F1 (Netzsch) with heating of 15 °C/min under an $N_2$ environment up to 1000 °C.

#### 2.2.6. Microstructure analysis

Scanning Electron Microscopy (SEM) was performed on a powder sample Phenom Pro-X and Thermo Fisher Scientific Quanta 200 3DFEG scanning electron microscope. The powder sample was spread on a carbon conductive adhesive tap followed by gold sputtering. Micrographs were recorded using a backscattered electron detector (BSE) at 15 kV with a spot of four.

#### 2.2.7. Leaching analysis

One batch leaching test was performed on the raw material and 28 days cured mortar sample according to EN-12457 using deionized water with a liquid-to-solid ratio of 10. The mixture was placed in plastic bottles and shaken continuously for 24 h at 21 ± 2 °C. After the experiment, the liquids were filtered through a 0.2 μm Polyether sulfone membrane and stored at 5 °C after acidifying with nitric acid (65% supra pure) to prevent precipitation. Before acidification, the pH was measured. An ICP-OES spectrometer (Spectroblue FMX36) was used for quantitative analysis of the leachate.

## 3. Results and discussion

### 3.1. Workability and its correlation with early age hydration

The spread flow of fresh mortar with different BCSA-slag compositions was adjusted in a way to attain approximate consistent flowability as presented in Fig. 2. For this purpose, the mixture with 50% slag was opted for since it presents the highest flowability due to the low water demand of the BOF slag (Kourounis et al., 2007; Liu and Li, 2014). The remaining BCSA-slag (0–40%) composition was adjusted by the addition of a superplasticizer to achieve a consistent ~20 ± 0.5 cm slump flow (Fig. 2 (a)). The substitution of slag in BCSA improves not only the flowability but also delays the final setting time from 45 to 85 min for the 0–30% BOF slag replacement as shown in Fig. 2 (b). The 30% slag addition in BCSA exhibited the highest delay in the setting time, and the further substitution (40 and 50%) did not further improve the setting time of the mixture. The improvement in the setting time of BCSA by substitution of the slag could help in diversifying its application (Quillin, 2001; Telesca et al., 2020).

To understand the mechanism of the slag contribution toward improving the workability of the BCSA-slag composite, a detailed thermal analysis was performed on the BCSA-slag paste with the same composition as used for mortar alongside the same water-to-binder (0.5) ratio. The 7 day heat of hydration is determined by isothermal calorimetry as shown in Fig. 2 (b, c). The first main exothermic heat of hydration maxima appears around 3 h in BCSA as well as 0–50% substitution of the slag sample. Peak 1 is attributed to the precipitation of tricalcium sulfoaluminate hydrate ($C_6A_3\overline{S}H_{32}$, ettringite, AFt) due to a rapid reaction of ye'elimite ($C_4A_3\overline{S}$) with water in the adequate amount of gypsum ($C\overline{S}H_2$) (1) (Liao et al., 2020):

$$C_4A_3\overline{S} + C\overline{S}H_2 + 34H \rightarrow C_6A\overline{S}_3H_{32} + 2AH_3 \quad (1)$$

As the amount of sulfate decreases in the solution, the peak 2 maxima appear around 6 h due to calcium monosulfoaluminate hydrate ($C_4A\overline{S}H_{12}$, AFm) precipitation upon depletion of gypsum (2) (Hargis et al., 2017):

$$C_4A_3\overline{S} + 18H \rightarrow C_4A\overline{S}H_{12} + 2AH_3 \quad (2)$$

After the ~14 h activity, BCSA cement, and the slag replacement clusters undergo a dormant period apparently, and no further exothermic hydration activity was observed. The 10% slag substitution in BCSA decreases the formation of AFt while promoting the formation of AFm phases as compared to BCSA due to the depletion of gypsum in the solution (Fig. 2 (c)). The further increase from 10 to 50% slag substitution decreases the formation of AFt as well as AFm phases. The cumulative heat release exhibited a significant downward trend upon

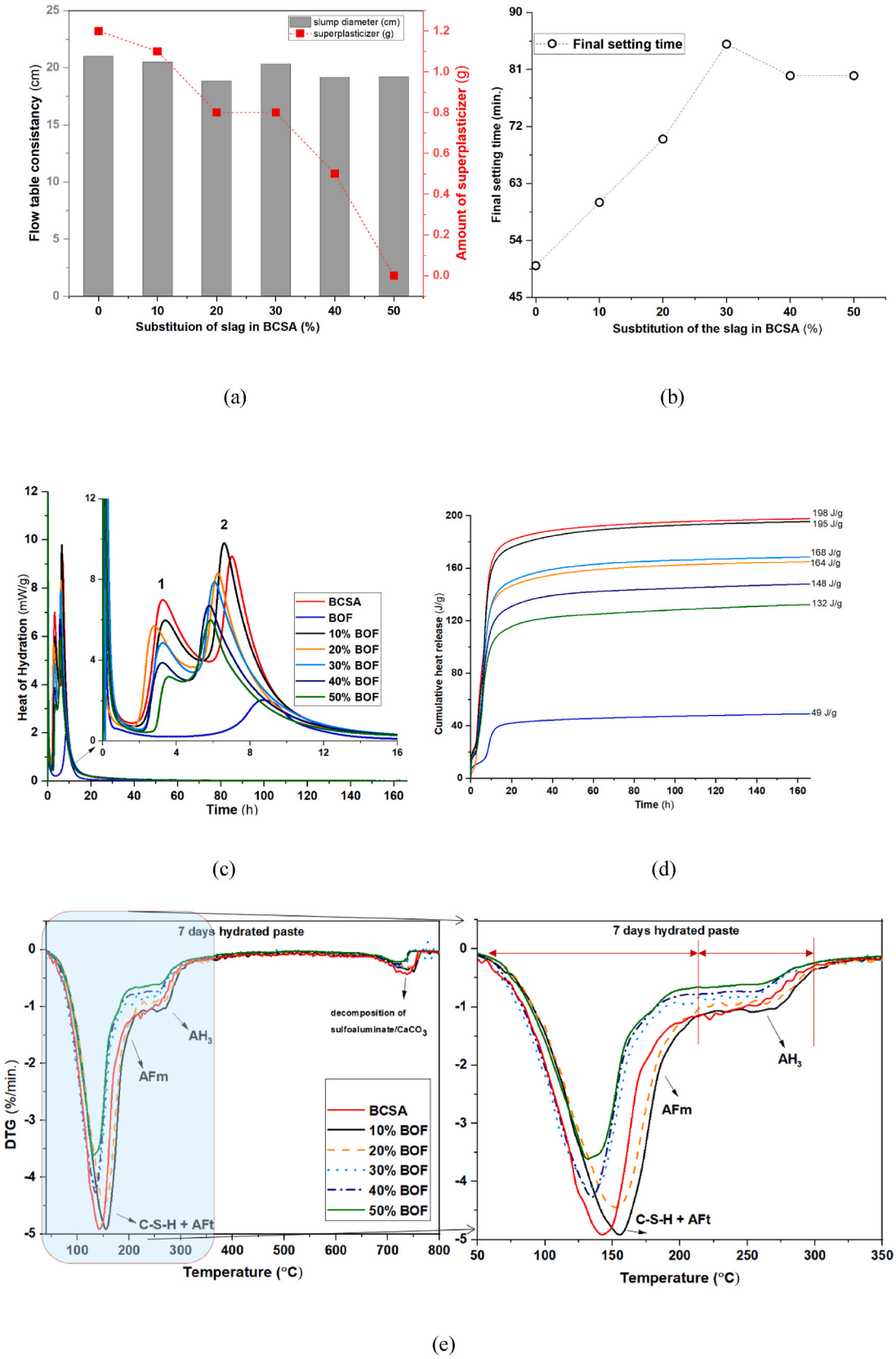


**Fig. 2.** Workability of BCSA-slag mortar (a) consistency of flowability of fresh mortar determined by flow table (diameter) and amount of superplasticizer (b) final setting of fresh mortar determined by Vicat needle test. Thermal analysis BCSA-slag pastes sample with 0–50% BOF slag substitution in BCSA cement (c) heat of hydration (d) cumulative heat of hydration (e) DTG analysis of 7 days cured sample (in the inset, the zoomed version of important mass loss events).

20–50% slag substitution in BCSA from 200 to ~130 J/g until 7 days (Fig. 2 (d)). The type of hydration products in 7 days of cured BCSA-slag pastes is further confirmed by derivative thermogravimetry (DTG) as shown in Fig. 2 (e) (see Fig. S1 (a) for percentage mass loss). The overlapping peaks <215 °C can be attributed largely to the dehydration of ettringite (AFt), monosulfoaluminate hydrate (AFm) alongside a small amount of C–S–H type phase. The mass loss event ~220–300 °C is attributed to the decomposition of amorphous aluminum hydroxide ($AH_3$). The mass loss event around ~700–800 °C attributed decarbonation of calcium carbonate as well as the decomposition of sulfoaluminates (Chi et al., 2021; Feng and Sun, 2020; Zhang et al., 2021). The mass loss maxima shift toward low corresponding $T_{max}$ <160 °C and peaks become sharper upon 30–40% replacement (Fig. 2 (e)) indicates that the presence of less variability of hydration products among Aft, Afm, and C–S–H type phases. The mass loss events confirmed that the 10–50% slag substitution in BCSA is contributing significantly to decreasing the amount of chemical-bound water leading to a negative effect on early hydration reaction.

It is clear from the thermal analysis that the 10–50% substitution of slag delays the setting time by inhibiting the early reactivity of BCSA (Fig. 2). It is important to mention here that the addition of slag does not delay the hydration reaction of BCSA but decreases the degree of hydration. Moreover, the early-stage (7 days) BCSA-slag composite reactivity is dominated by the BCSA reactivity, and the BOF slag contributes as a dilution effect (Chi et al., 2021). This shows that it is necessary to investigate the long-term BCSA-slag cured sample to observe the possible improved mechanical performance.

### 3.2. Mechanical performance and correlation with BCSA-slag hydration

Mechanical performance of the mortar specimens tested at ages 1,3, 7, 28, 90, and 180 days has been shown in Fig. 3 (see Figs. S2(a and b) for percentage flexural and compressive strength results respectively). The BCSA replacement with BOF slag exhibited a decrease in flexural strength till 28 days except for the 50% BOF sample. At 90 days, 20–50% BOF slag samples exhibited an improvement in flexural strength. Upon curing for 180 days, all BOF slag replacement samples attained higher flexural strength than 100% BCSA (REF) cement. So, the 30% slag replacement in BCSA cement provides the best flexural resistance after 6 months of curing (Fig. 3 (a)).

As the 10% of BCSA cement was replaced by the BOF slag in 10% BOF, a slight decrease up to ~11% in the compressive strength was observed till 28 days as compared to REF specimens (Fig. 3 (b)). The decrease in the compressive strength becomes more pronounced ~18% at 90 and 180 days of curing of the mortar sample. A clear decrease from ~25 to 46% in the compressive strength of 20–50% BOF samples as compared to the BCSA specimen was observed at 28 days. At 90 days, the 30–50% BOF slag sample exhibited a clear increase in compression resistance, and the 40% BOF sample reached ~33 MPa similar to the REF (~32 MPa) sample. At 180 days, the compressive strength of 30–50% BOF samples reaches ~60, 55, and 46 MPa, respectively, as compared to REF ~43 MPa (Fig. 3(b)). The flexural strength of the 30% BOF sample reaches 9.1 MPa with the highest compressive strength of 60.3 MPa at 180 days Fig. 3(a and b). A decrease in the mechanical performance at later stages is reported upon the addition of steel slag in calcium sulfoaluminate cement (Liao et al., 2020). However, the present study exhibited a promise for 30–50% BOF slag substitution.

To get insight into the mechanical performance, the hydration products BCSA-mortar specimens were analyzed by XRD as well as thermal gravimetric analysis. The diffraction pattern of the BSCA-slag specimens has been shown in Fig. 4 (a, b). At 28 days, the crystalline hydration products were dominated by ettringite, quartz, and calcite alongside the gibbsite. At 90 days, more crystalline hydration products such as strätlingite and Fe-katoite alongside the main hydration products of BCSA cement were observed. The labeled peak of strätlingite and Fe-katoite can also be assigned to the layered double-hydroxides (LDH) like compounds containing $CO_3^{2-}$, $OH^-$, and $Cl^-$ ions (Borštnar et al., 2021). Moreover, the diffraction analysis was performed on the mortar sample that requires mechanical grinding and relatively high-intensity quartz peaks leading to the inherent problem of undermining the presence of semi-crystalline or nanocrystalline hydration products. Therefore, the hydration products are further confirmed through DTG as shown in Fig. 4 (see Fig. S1 (b, c, d, e, f) for percentage mass loss). The 1, 3, and 7 days cured mortar samples exhibited the mass loss event around ~60–220 °C corresponding to the thermal dehydration of the AFt, AFm as well as C–S–H partially. While the mass loss event ~230–300 °C attributed to the dehydration of gibbsite ($AH_3$) (Fig. 4 (c, d, e)). At 28 days, a new mass loss event centered at ~175 °C which corresponds to the dehydration of strätlingite ($C_2ASH_8$) as evident in the 40 and 50% BOF samples (Fig. 4 (f)) (Jeong et al., 2018). Upon further curing till 90 days, a new mass loss event ~300–420 °C associated with the dehydration of katoite (hydrogarnet) alongside strätlingite ($C_2ASH_8$) was observable in 20, 30, 40, and 50% BOF samples (Fig. 4 (g)) (Kaja et al., 2021). The presence of katoite and strätlingite was not observed in REF,

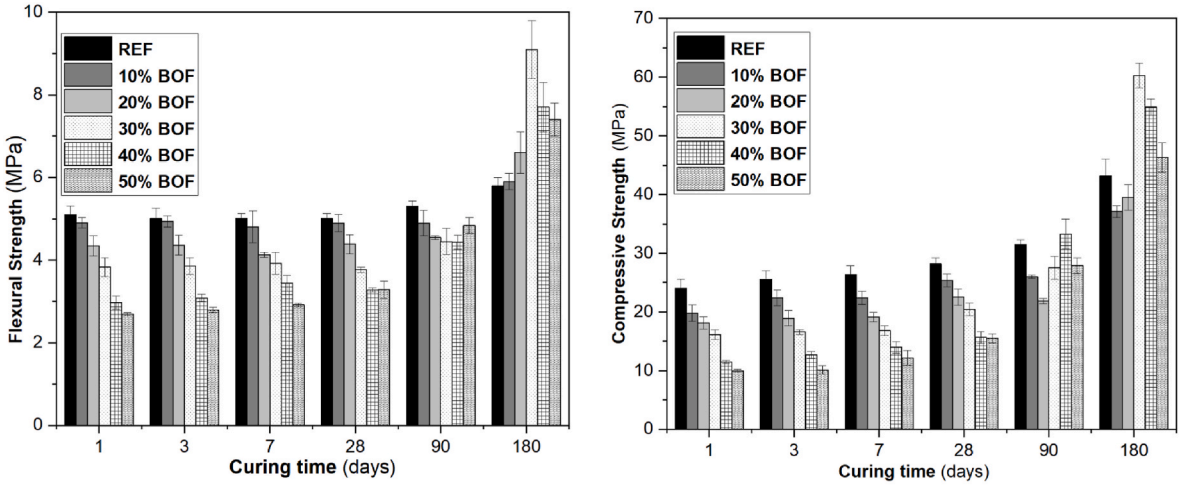


**Fig. 3.** Mechanical performance of BSCA-slag mortar specimens containing 0–50% substitution of air granulated BOF slag (a) flexural and (b) compressive strength.

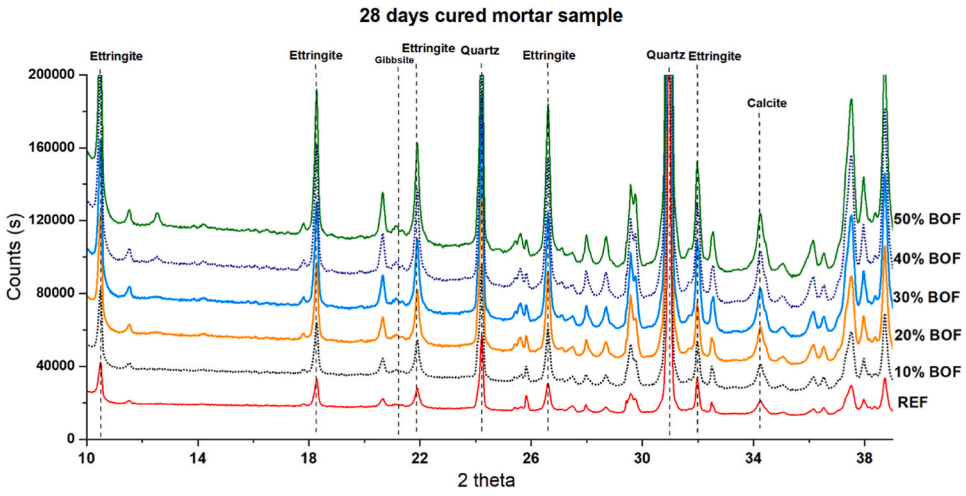


(a)

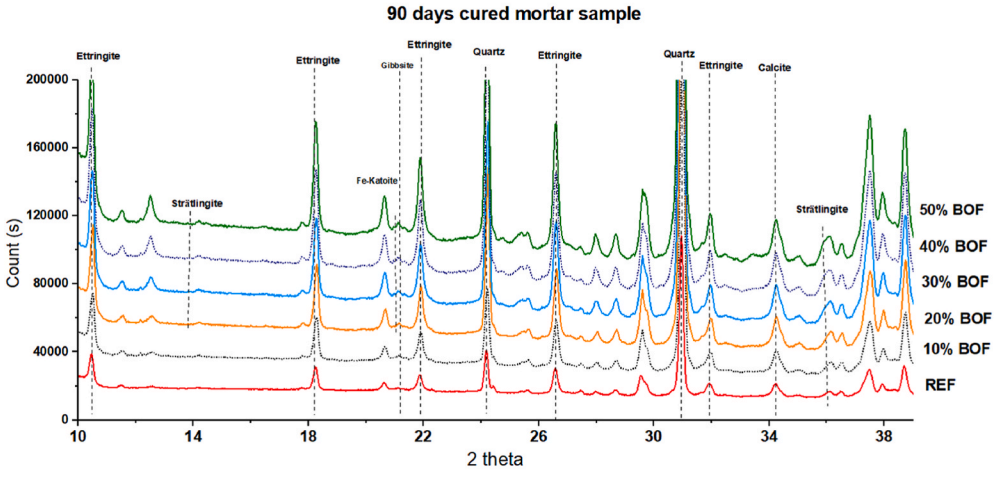


(b)

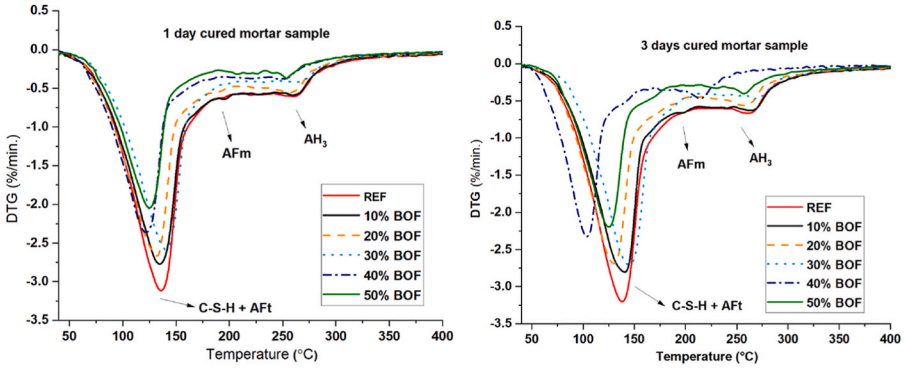


(c) (d)

**Fig. 4.** The labeled peak diffractogram of BCSA-slag mortar specimens containing 0–50% substitution of air granulated BOF slag (a) 28 days cured mortar sample (b) 90 days cured mortar sample. Derivative thermogravimetry (DTG) of BSCA-slag mortar specimens containing 0–50% substitution of air granulated BOF slag (c) 1 (d) 3 (e) 7 (f) 28 and (g) 90 days cured mortar samples.

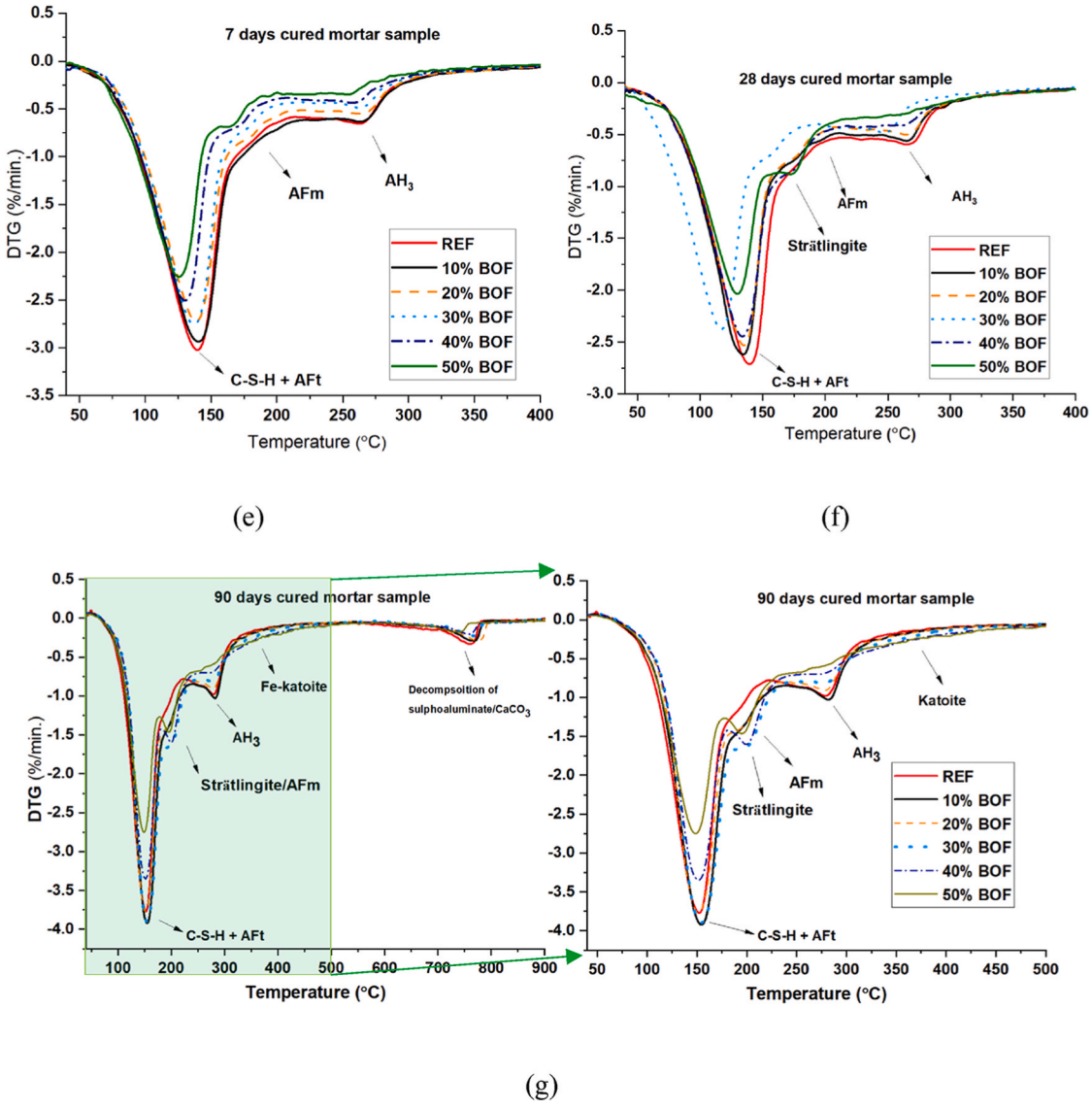


**Fig. 4.** (*continued*).

10% BOF samples. The $C_2S$ tends to form strätlingite under an alumina-rich environment (3) (Chi et al., 2021):

$$C_2S + AH_3 + 5H \rightarrow C_2ASH_8 \quad (3)$$

Moreover, the katoite hydrogarnet is the product of the brownmillerite reaction. It is clear from the hydration product of BCSA-slag mortar clusters that the brownmillerite alongside $C_2S$ also contributes toward reactivity in 30–50% BOF samples leading to improved compressive and flexural strength at 90 days (Fig. 3 (a, b)). While these phases did not show significant reactivity in BCSA cement, 10 and 20% BOF samples till 90 days of curing. Among all these samples, the 30% slag replacement cluster is recommended for the best performance at a later age (28–180 days).

### 3.3. Microstructure analysis

The SEM-BS (backscattered images) of 7 and 28 days cured BSCA-slag specimens have been presented in Fig. 5. The rod-like crystals of AFt covered with colloidal and spherical $AH_3$ gel structures to form a skeleton during the hydration of BCSA leading to the high strength of the BCSA sample (Fig. 5(a)). Upon 28 days of curing of REF mortar specimen, the hydration products such as AFt and amorphous intergrown colloidal $AH_3$ structure seem well distributed all over the mortar matrix, thereby providing high strength from an early age (1–28 days) hydration (Fig. 5(b)). The morphology of $AH_3$ precipitated particles depends on the gypsum ($C\overline{S}H_2$) concentration in the hydration media (Song et al., 2015). Upon 10% BOF slag replacement in BCSA, the irregular lamellar morphology AFm (less distinctive) intercalated with distinctive AFt observed with dominant colloidal $AH_3$ morphology (Fig. 5(c)). As the hydration progressed to 28 days, the 10% BOF mortar matrix contained a uniform distribution of AFt phases (Fig. 5(d)). A further 20–50% BOF slag in BCSA, a clear decrease in the AFt formation alongside a distinctive decrease in the formation of amorphous $AH_3$ formation (Fig. 5(e, f, g, h, i, j, k, l)). The decrease in the formation of AFt and amorphous $AH_3$ colloidal network reduces the binding between hydration products and the BCSA-slag matrix. Thereby, a decrease in mechanical performance slag substituted mortar is observed upon curing till 28 days (Fig. 3).

It is worth noticing that the formation of amorphous phases such as gibbsite ($AH_3$) contributes significantly to the mechanical stability of BCSA-slag binder. The 90 days cured mortar sample of 40 and 50% BOF sample showed a laminar particle of strätlingite alongside katoite well intergrown with the AFt, C–S–H, and gibbsite phases (Fig. 5 (m, n, o, p) (Santacruz et al., 2016). That's why, the 30–50% BOF replacement

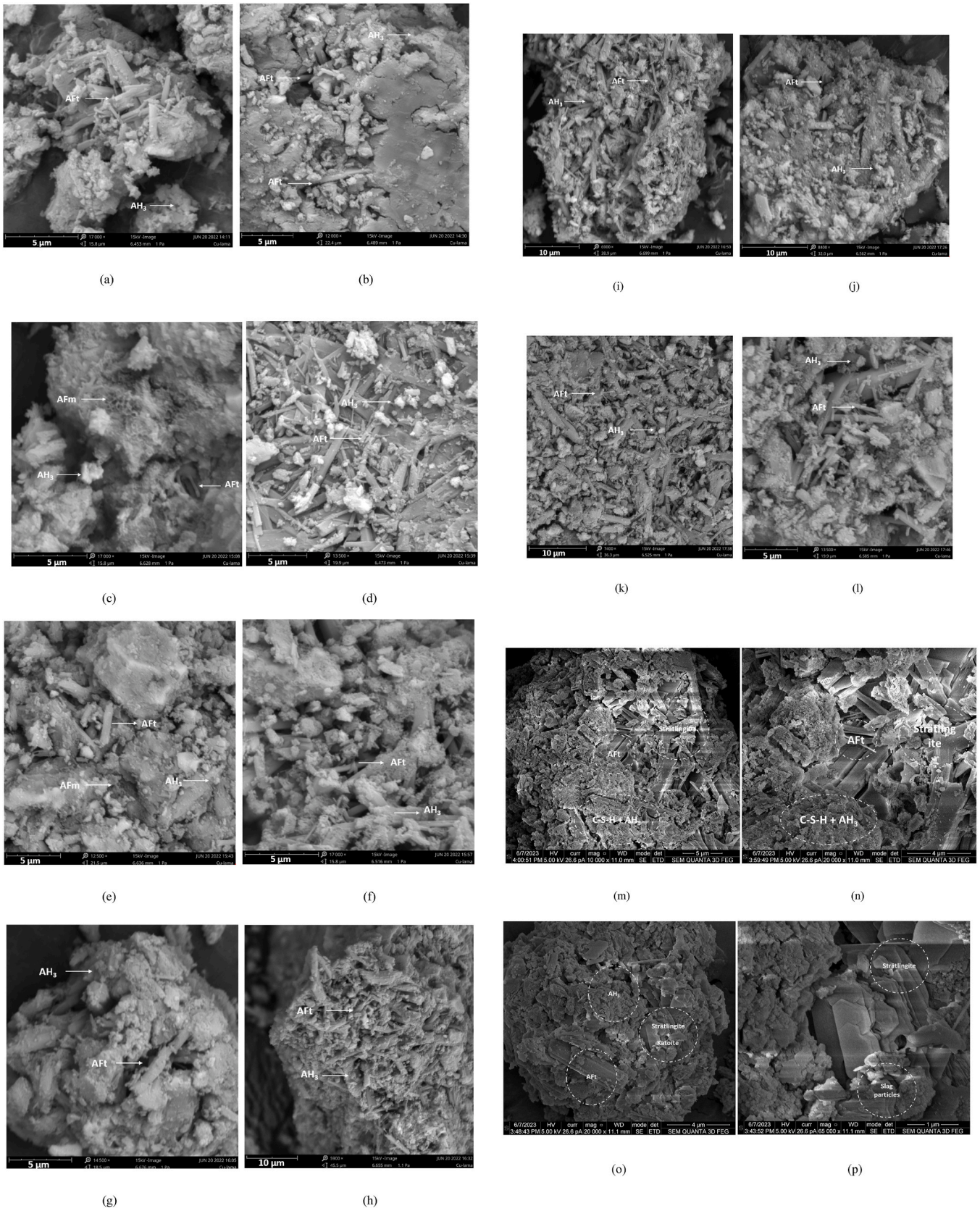


**Fig. 5.** SEM analysis of BSCA-slag specimens (a) 7 days cured BCSA paste sample (b) 28 days cured REF sample (c) 7 days cured 10% BOF paste sample (d) 28 days cured 10% BOF mortar sample (e) 7 days cured 20% BOF paste sample (f) 28 days cured 20% BOF mortar sample (g) 7 days cured 30% BOF paste sample (h) 28 days cured 30% BOF mortar sample (i) 7 days cured 40% BOF paste sample (j) 28 days cured 40% BOF mortar sample (k) 7 days cured 50% BOF paste sample (l) 28 days cured 50% BOF mortar sample (m, n) 90 days cured 50% BOF mortar sample (o, p) 90 days cured 40% BOF mortar sample.

exhibited better mechanical performance at 90 days due to equilibrium gibbsite and CSH-$C_2ASH_8$ formation which enhances the binding capacity of BCSA-slag composite (Figs. 2–4). So, the presence of an adequate amount of amorphous matrix is a prerequisite for the good mechanical resistance of BCSA-slag mortars.

### 3.4. Drying shrinkage and drying mass loss

The drying shrinkage tests were carried out to confirm the volumetric stability of BCSA due to the addition of air granulated BOF slag over 72 days as shown in Fig. 6 (a). The permissible limit for shrinkage on BCSA mortar should not exceed 750 μm at 28 days according to BCSA cement technical data sheet. In this regard, the highest length variation value found was ~675 μm at 28 days which is below the technical requirement of the cement. The absence of shrinkage is one of the assets of the BCSA against OPC (Sirtoli et al., 2020). The drying mass stability of the BCSA-slag mortar was measured as shown in Fig. 6 (b). The slag replacement in BCSA cement consistently increases the variation of mass loss till 28 days. Because the addition of slag acts as a dilution effect as explained in Section 3.2. After 28 days, the dicalcium silicate and brownmillerite phases also contribute toward the hydration reaction leading to the stabilization of water loss from the BCSA-slag mortar specimens. A high drying mass loss of ~3% in 50% BOF slag replacement is observed. Upon lowering the water-to-solid ratio, good mechanical performance can be achieved due to improved particle packing. In this way, the 50% slag can be substituted in BCSA cement (Chaurand et al., 2007).

### 3.5. Environmental impact

The leaching of BOF slag and BCSA cement (raw materials) as well as 28 days cured mortar sample has been presented in Table 3. The BCSA cement exhibited significantly higher Cr (2.3 ppm) leaching than the permissible limit (0.63 ppm). The air granulated BOF slag also releases slightly higher Cr (0.64 ppm) than the permissible limit. On the other hand, V leaching of the slag is below the permissible limit of the Dutch soil quality decree (Ahmed et al., 2023). Upon 28 days of curing, the REF mortar specimen Cr leaching reduced to 0.59 ppm which gradually decreased with every 10% BOF slag replacement (Table 3). In the case of V leaching, the slag replacement increased the leaching up to 1 ppm except for 50% BOF replacement. The variation of heavy metals leaching can be explained in terms of pH, mineral source, immobilization potential of hydration products, and kinetic equilibrium between varying oxides of chromate and vanadate.

As explained above in Sections 3.1 and 3.2, the main hydration product of BCSA is AFt which tends to immobilize the $CrO_4^{2-}$ in the molecular structure (Peysson et al., 2005). The replacement of BCSA with BOF slag decreases the Cr leaching partially due to the dilution effect of the slag as explained above. Moreover, the dominant chromate ion is $CrO_4^{2-}$ at pH 11.9–12.6 which has very low solubility ($K_{sp} = 5.1 \times 10^{-6}$). So, the Cr can also be immobilized partially by the formation of the low solubility complex. However, the BOF slag also contains a significant amount of leachable Cr (Table 3). It can be argued that the Cr leaching will be high at the curing age >28 days upon hydration of slag phases. However, the hydration products such as katoite (hydrogarnet) that form at later stages can also host high quantities of $Cr^{6+}$ alongside strätlingite, AFt, and AFm which would increase the immobilization potential of hydration media (Peysson et al., 2005; Piekkari et al., 2020). Regarding the air granulated BOF slag leaching, $V^{5+}$ tends to occupy the Si-site in $C_2S$ in BOF slag (Hobson et al., 2017). So, the dissolution of $C_2S$ also increases the chances of V release in the leachate. $Ca_3(VO_4)_2$ ($logK_{sp} = -17.97$) is the dominant precipitate at pH = 11.9–12.6 that is insoluble at room temperature (Spooren et al., 2016). The equilibrium formation of C–S–H phases with $C_2S$ dissolution would permit the high $Ca^{2+}$ concentration in the leachate which limits the solubility of $Ca_3(VO_4)_2$ (Neuhold et al., 2019). Moreover, C–S–H can also actively uptake some parts of $V_2O_5$ on tetrahedral Si-sites. As explained above in Section 3.2, $C_2S$ actively takes part in hydration reaction at curing age >28 days in 30–50% BOF samples. So, the BCSA-composite provides a way to avoid leaching in the novel binder.

This study provides a basis for the valorization of air granulated BOF slag in BCSA cement where a high replacement of ~30–50% can be warranted. This study shows that air granulated slag provides good stability, and variability in setting time to belite calcium sulfoaluminate cement which could help diversify its application in concrete. The mechanical and chemical activation of the slag approaches can be employed successfully to improve the mechanical performance of the new BCSA-slag binder at an early stage which is a concern for effective utilization of the BOF slag. Moreover, the concern of ground/surface water pollution considering the Cr leaching needs to be addressed in the follow-up study by analyzing the long-term leaching behaviour, particularly upon carbonation as well as at demolished concrete stage. The air granulated BOF slag as an ideal match for the BCSA substitution was the main aim of this study.

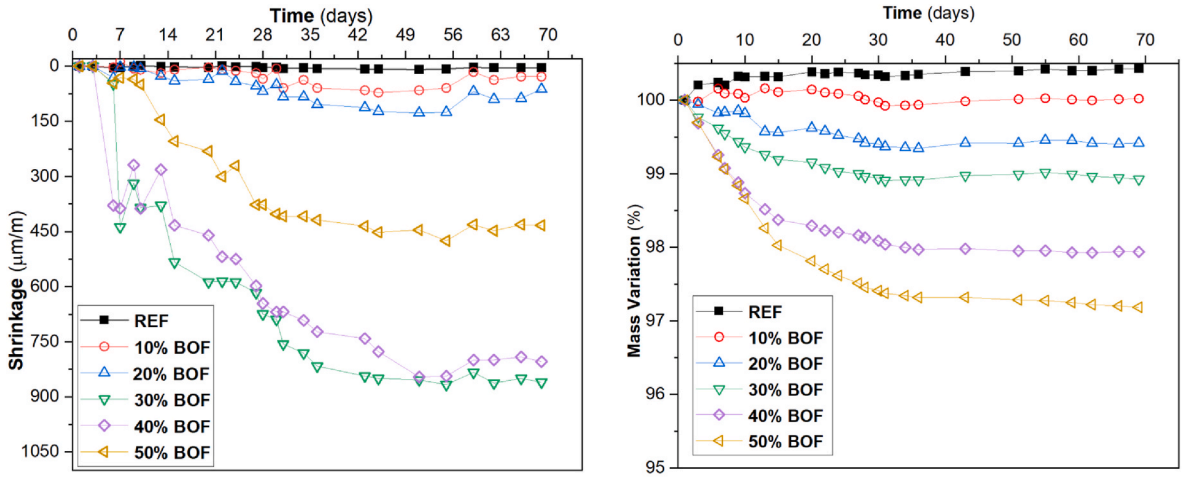


(a) (b)

**Fig. 6.** BSCA-slag mortar specimens containing 0–50 % substitution of air granulated BOF slag (a) length variation (b) mass variation.

**Table 3**
One batch leaching (NEN: 1245-7) analysis of raw material and 28 days cured mortar sample.

| Sample | legal limits | BOF slag | BCSA cement | REF | 10% BOF | 20% BOF | 30% BOF | 40% BOF | 50% BOF |
|---|---|---|---|---|---|---|---|---|---|
| pH | | 12.6 | 11.9 | 11.9 | 11.9 | 11.9 | 12.1 | 12.1 | 12.2 |
| Elements (ppm) | | | | | | | | | |
| Al | - | 7.5 | 282.1 | 242.2 | 123 | 145.1 | 245.3 | 215.1 | 142.5 |
| Ba | 22 | 1.2 | 0.5 | 0.1 | 0.3 | 0.1 | 0.1 | 0.1 | 0.1 |
| Cr | 0.63 | 0.64 | 2.3 | 0.6 | 0.48 | 0.43 | 0.39 | 0.31 | 0.29 |
| Fe | - | 0.3 | 17.6 | 3.9 | 3.8 | 3.8 | 2.9 | 2.4 | 1.7 |
| Si | - | 26.9 | 24.5 | 17.3 | 22.7 | 22.2 | 13.1 | 13.2 | 18 |
| V | 1.8 | 0.4 | 0.1 | 0.0 | 0.7 | 0.9 | 1.2 | 1 | 0.4 |

*Sb, As, Cu, Co, Hg, Ni, Se, Cd, Pb, and Sn were below the detection limit.

In Europe, research has focused on the "Belite-Yeélimite-Ferrite" (BYF) clinkers containing belite as major content alongside ferrite ($C_4AF$), and ye'elimite content below 35% (Scrivener et al., 2018). Therefore, the manufacturers require much smaller amounts of the most expensive aluminum-rich raw materials than conventional calcium sulfoaluminate cement. The BOF slag is a good source of belite and ferrite phases which can be used alongside BYF clinker. BYF clinkers (e.g., "Aether" or "Ternocem") have the potential to replace Portland cement clinker as well as Portland-slag cement in many applications with a $CO_2$ saving of 20% per unit of clinker in the cement approximately. Using 30–50% BOF slag as a kiln feed or in mortar application would help mitigate the challenge of high raw material costs to the commercialization of BYF technology. Moreover, it would also help to achieve the sustainability goals set by the Netherlands.

## 4. Conclusions

In this study, the standard mortar specimens with 0, 10, 20, 30, 40, and 50% air granulated BOF slag as for BCSA were investigated for the workability, mechanical performance, drying mass, and length variation as well as immobilization of heavy metals in relations with the degree of hydration and type of hydration products.

- The main hydration products are ettringite, monosulphoaluminate hydrate, and aluminum hydroxide with C–S–H phase partially alongside strätlingite and katoite due to dicalcium silicate and brownmillerite reactivity.
- At an early age (1–28 days), the 10–50% slag acts as a dilution effect which decreases the degree of hydration of BCSA-slag mortar leading to a delay in final setting time and decreasing mechanical performance at an early age. At 180 days, the 30–50% BOF replacement clusters showed better mechanical performance than 100% BCSA cement with the 30% BOF slag replacement cluster providing the highest flexural and compressive strength of ~9.1 and 60.3 MPa, respectively.
- The better mechanical of 30–50% slag mortars can be attributed to the formation of equilibrium gibbsite and CSH-$C_2ASH_8$ semi-crystalline amorphous matrix together with katoite, ettringite, calcium monosulfoaluminate hydrate which enhances the binding capacity between BSCA-slag specimens.
- The drying shrinkage of all BCSA-slag specimens does not exceed the permissible limit of 750 μm/m at 28 days. Moreover, a high drying mass loss of ~3% in 50% BOF slag replacement indicates that the water-to-solid ratio can be lowered to get good mechanical performance.
- All BCSA-slag mortar specimens exhibited the Cr and V leaching below the permissible limit according to the Dutch soil quality decree.

## CRediT authorship contribution statement

**Muhammad Jawad Ahmed:** Conceptualization, Data curation, Formal analysis, Investigation, Methodology, Software, Supervision, Validation, Visualization, Writing – original draft. **Sterenn Durand:** Conceptualization, Formal analysis, Investigation, Methodology, Software, Validation, Visualization. **Marc Antoun:** Methodology, Project administration, Supervision, Writing – review & editing. **Florent Gauvin:** Conceptualization, Formal analysis, Investigation, Project administration, Supervision, Writing – review & editing. **Sofiane Amziane:** Formal analysis, Investigation, Methodology, Project administration, Supervision, Writing – review & editing. **H.J.H. Brouwers:** Conceptualization, Funding acquisition, Methodology, Project administration, Resources, Supervision, Writing – review & editing.

## Declaration of competing interest

The authors declare that they have no known competing financial interests or personal relationships that could have appeared to influence the work reported in this paper.

## Data availability

Data will be made available on request.

## Acknowledegment

The authors would like to acknowledge the financial support by NWO (The Netherlands Organisation for Scientific Research) for funding this research (project no.10023338) and M2i (Materials Innovation Institute, project no. S81.6.15565b) for managing this project. Furthermore, the authors wish to express their gratitude to the following sponsors of this research: Tata Steel; Vicat Cement; ENCI; V.d. Bosch Beton; Blue Phoenix Group; Hess.

## Appendix A. Supplementary data

Supplementary data to this article can be found online at https://doi.org/10.1016/j.jclepro.2023.140539.

## References

Ahmed, M.J., Cuijpers, R., Schollbach, K., Van Der Laan, S., Van Wijngaarden-Kroft, M., Verhoeven, T., Brouwers, H.J., 2023. V and Cr substitution in dicalcium silicate under oxidizing and reducing conditions – Synthesis, reactivity, and leaching behavior studies. J. Hazard Mater. 442, 130032 https://doi.org/10.1016/J.JHAZMAT.2022.130032.

Benhelal, E., Zahedi, G., Shamsaei, E., Bahadori, A., 2013. Global strategies and potentials to curb CO2 emissions in cement industry. J. Clean. Prod. 51, 142–161. https://doi.org/10.1016/j.jclepro.2012.10.049.

Borštnar, M., Lengauer, C.L., Dolenec, S., 2021. Quantitative in situ X-ray diffraction analysis of early hydration of belite-calcium sulfoaluminate cement at various Defined temperatures. Minerals 11, 297. https://doi.org/10.3390/min11030297.

Chaurand, P., Rose, J., Briois, V., Salome, M., Proux, O., Nassif, V., Olivi, L., Susini, J., Hazemann, J.-L., Bottero, J.-Y., 2007. New methodological Approach for the vanadium K-Edge X-ray Absorption Near-Edge structure Interpretation: application to the Speciation of vanadium in oxide phases from steel slag. J. Phys. Chem. B 111, 5101–5110. https://doi.org/10.1021/jp063186i.

Chen, X., Li, J., Lu, Z., Ng, S., Niu, Y., Jiang, J., Xu, Y., Lai, Z., Liu, H., 2022. The role of brownmillerite in preparation of high-belite sulfoaluminate cement clinker. Appl. Sci. 12, 4980. https://doi.org/10.3390/app12104980.

Chi, L., Wang, Z., Lu, S., Wang, H., Liu, K., Liu, W., 2021. Early assessment of hydration and microstructure evolution of belite-calcium sulfoaluminate cement pastes by electrical impedance spectroscopy. Electrochim. Acta 389, 138699. https://doi.org/10.1016/J.ELECTACTA.2021.138699.

De Windt, L., Chaurand, P., Rose, J., 2011. Kinetics of steel slag leaching: batch tests and modeling. Waste Manag. 31, 225–235. https://doi.org/10.1016/j.wasman.2010.05.018.

Eloneva, S., 2010. Reduction of CO2 Emissions by Mineral Carbonation: Steelmaking Slags and Raw Material with a Pure Calcium Carbonate End Product. TKK Diss.

Engström, F., Adolfsson, D., Yang, Q., Samuelsson, C., Björkman, B., 2010. Crystallization behaviour of some steelmaking slags. Steel Res. Int. 81, 362–371. https://doi.org/10.1002/SRIN.200900154.

Favier, A., De Wolf, C., Scrivener, K., Habert, G., 2018. A Sustainable Future for the European Cement and Concrete Industry. https://doi.org/10.3929/ethz-b-000301843.

Feng, J., Sun, J., 2020. A comparison of the 10-year properties of converter steel slag activated by high temperature and an alkaline activator. Constr. Build. Mater. 234, 116948 https://doi.org/10.1016/j.conbuildmat.2019.116948.

Guo, J., Bao, Y., Wang, M., 2018. Steel slag in China: Treatment, recycling, and management. Waste Manag. https://doi.org/10.1016/j.wasman.2018.04.045.

Hargis, C.W., Lothenbach, B., Müller, C.J., Winnefeld, F., 2017. Carbonation of calcium sulfoaluminate mortars. Cem. Concr. Compos. 80, 123–134. https://doi.org/10.1016/j.cemconcomp.2017.03.003.

Hargis, C.W., Telesca, A., Monteiro, P.J.M., 2014. Calcium sulfoaluminate (Ye'elimite) hydration in the presence of gypsum, calcite, and vaterite. Cem. Concr. Res. 65, 15–20. https://doi.org/10.1016/j.cemconres.2014.07.004.

Hobson, A.J., Stewart, D.I., Bray, A.W., Mortimer, R.J.G., Mayes, W.M., Rogerson, M., Burke, I.T., 2017. Mechanism of vanadium leaching during surface weathering of basic oxygen furnace steel slag Blocks: a Microfocus X-ray Absorption spectroscopy and electron microscopy study. Environ. Sci. Technol. 51, 7823–7830. https://doi.org/10.1021/acs.est.7b00874.

Horii, K., Tsutsumi, N., Kitano, Y., Kato, T., 2013. Processing and reusing technologies for steelmaking slag. Nippon Steel Tech. Rep.

Iacobescu, R.I., Pontikes, Y., Koumpouri, D., Angelopoulos, G.N., 2013. Synthesis, characterization and properties of calcium ferroaluminate belite cements produced with electric arc furnace steel slag as raw material. Cem. Concr. Compos. 44, 1–8. https://doi.org/10.1016/j.cemconcomp.2013.08.002.

Jawad Ahmed, M., Franco Santos, W., Brouwers, H.J.H., 2023. Air granulated basic Oxygen furnace (BOF) slag application as a binder: effect on strength, volumetric stability, hydration study, and environmental risk. Constr. Build. Mater. 367, 130342 https://doi.org/10.1016/j.conbuildmat.2023.130342.

Jeong, Y., Hargis, C.W., Chun, S.-C., Moon, J., 2018. The effect of water and gypsum content on strätlingite formation in calcium sulfoaluminate-belite cement pastes. Constr. Build. Mater. 166, 712–722. https://doi.org/10.1016/j.conbuildmat.2018.01.153.

Jiang, Y., Ling, T.C., Shi, C., Pan, S.Y., 2018. Characteristics of steel slags and their use in cement and concrete—a review. Resour. Conserv. Recycl. 136, 187–197. https://doi.org/10.1016/J.RESCONREC.2018.04.023.

Kaja, A.M., Schollbach, K., Melzer, S., van der Laan, S.R., Brouwers, H.J.H., Yu, Q., 2021. Hydration of potassium citrate-activated BOF slag. Cem. Concr. Res. 140, 106291 https://doi.org/10.1016/j.cemconres.2020.106291.

Kourounis, S., Tsivilis, S., Tsakiridis, P.E., Papadimitriou, G.D., Tsibouki, Z., 2007. Properties and hydration of blended cements with steelmaking slag. Cem. Concr. Res. 37, 815–822. https://doi.org/10.1016/j.cemconres.2007.03.008.

Li, Y., Dai, W. Bin, 2018. Modifying hot slag and converting it into value-added materials: a review. J. Clean. Prod. 175, 176–189. https://doi.org/10.1016/J.JCLEPRO.2017.11.171.

Liao, Y., Jiang, G., Wang, K., Al Qunaynah, S., Yuan, W., 2020. Effect of steel slag on the hydration and strength development of calcium sulfoaluminate cement. Constr. Build. Mater. 265, 120301 https://doi.org/10.1016/j.conbuildmat.2020.120301.

Link, T., Bellmann, F., Ludwig, H.M., Ben Haha, M., 2015. Reactivity and phase composition of Ca2SiO4 binders made by annealing of alpha-dicalcium silicate hydrate. Cem. Concr. Res. 67, 131–137. https://doi.org/10.1016/j.cemconres.2014.08.009.

Liu, C., Huang, S., Blanpain, B., Guo, M., 2019. Effect of Al2O3 addition on mineralogical modification and Crystallization kinetics of a high Basicity BOF steel slag. Metall. Mater. Trans. B 50, 271–281. https://doi.org/10.1007/s11663-018-1465-7.

Liu, S., Li, L., 2014. Influence of fineness on the cementitious properties of steel slag. J. Therm. Anal. Calorim. 117, 629–634. https://doi.org/10.1007/s10973-014-3789-0.

Ludwig, H.M., Zhang, W., 2015. Research review of cement clinker chemistry. Cem. Concr. Res. https://doi.org/10.1016/j.cemconres.2015.05.018.

Martins, A.C.P., Franco de Carvalho, J.M., Duarte, M. do N., Lima, G.E.S. de, Pedroti, L. G., Peixoto, R.A.F., 2022. Influence of a LAS-based modifying admixture on cement-based composites containing steel slag powder. J. Build. Eng. 53, 104517 https://doi.org/10.1016/j.jobe.2022.104517.

Neuhold, S., van Zomeren, A., Dijkstra, J.J., van der Sloot, H.A., Drissen, P., Algermissen, D., Mudersbach, D., Schüler, S., Griessacher, T., Raith, J.G., Pomberger, R., Vollprecht, D., 2019. Investigation of possible leaching control mechanisms for chromium and vanadium in electric arc furnace (EAF) slags using Combined experimental and modeling approaches. Minerals. https://doi.org/10.3390/min9090525.

Peysson, S., Péra, J., Chabannet, M., 2005. Immobilization of heavy metals by calcium sulfoaluminate cement. Cem. Concr. Res. 35, 2261–2270. https://doi.org/10.1016/J.CEMCONRES.2005.03.015.

Piekkari, K., Ohenoja, K., Isteri, V., Tanskanen, P., Illikainen, M., 2020. Immobilization of heavy metals, selenate, and sulfate from a hazardous industrial side stream by using calcium sulfoaluminate-belite cement. J. Clean. Prod. 258, 120560 https://doi.org/10.1016/j.jclepro.2020.120560.

Quillin, K., 2001. Performance of belite–sulfoaluminate cements. Cem. Concr. Res. 31, 1341–1349. https://doi.org/10.1016/S0008-8846(01)00543-9.

Santacruz, I., Torre, Á.G.D. la, Álvarez-Pinazo, G., Cabeza, A., Cuesta, A., Sanz, J., Aranda, M.A.G., 2016. Structure of stratlingite and effect of hydration methodology on microstructure. Adv. Cem. Res. 28, 13–22. https://doi.org/10.1680/adcr.14.00104.

Santos, W.F., Schollbach, K., Melzer, S., van der Laan, S.R., Brouwers, H.J.H., 2023. Quantitative analysis and phase assemblage of basic oxygen furnace slag hydration. J. Hazard Mater. 131029 https://doi.org/10.1016/J.JHAZMAT.2023.131029.

Schneider, M., Romer, M., Tschudin, M., Bolio, H., 2011. Sustainable cement production—present and future. Cem. Concr. Res. 41, 642–650. https://doi.org/10.1016/j.cemconres.2011.03.019.

Schollbach, K., Ahmed, M.J., van der Laan, S.R., 2021. The mineralogy of air granulated converter slag. Int. J. Ceram. Eng. Sci. 3, 21–36. https://doi.org/10.1002/ces2.10074.

Scrivener, K.L., John, V.M., Gartner, E.M., 2018. Eco-efficient cements: potential economically viable solutions for a low-CO2 cement-based materials industry. Cem. Concr. Res. 114, 2–26. https://doi.org/10.1016/j.cemconres.2018.03.015.

Shen, H., Forssberg, E., 2003. An overview of recovery of metals from slags. Waste Manag. 23, 933–949. https://doi.org/10.1016/S0956-053X(02)00164-2.

Shen, W., Cao, L., Li, Q., Zhang, W., Wang, G., Li, C., 2015. Quantifying CO2 emissions from China's cement industry. Renew. Sustain. Energy Rev. 50, 1004–1012. https://doi.org/10.1016/j.rser.2015.05.031.

Sirtoli, D., Wyrzykowski, M., Riva, P., Lura, P., 2020. Autogenous and drying shrinkage of mortars based on Portland and calcium sulfoaluminate cements. Mater. Struct. 53, 126. https://doi.org/10.1617/s11527-020-01561-1.

Song, F., Yu, Z., Yang, F., Lu, Y., Liu, Y., 2015. Microstructure of amorphous aluminum hydroxide in belite-calcium sulfoaluminate cement. Cem. Concr. Res. 71, 1–6. https://doi.org/10.1016/j.cemconres.2015.01.013.

Spooren, J., Kim, E., Horckmans, L., Broos, K., Nielsen, P., Quaghebeur, M., 2016. In-situ chromium and vanadium recovery of landfilled ferrochromium and stainless steel slags. Chem. Eng. J. 303, 359–368. https://doi.org/10.1016/j.cej.2016.05.128.

Telesca, A., Matschei, T., Marroccoli, M., 2020. Study of Eco-Friendly belite-calcium sulfoaluminate cements obtained from special wastes. Appl. Sci. 10, 8650. https://doi.org/10.3390/app10238650.

Tsakiridis, P.E., Papadimitriou, G.D., Tsivilis, S., Koroneos, C., 2008. Utilization of steel slag for Portland cement clinker production. J. Hazard Mater. 152, 805–811. https://doi.org/10.1016/J.JHAZMAT.2007.07.093.

Wulfert, H., Ludwig, H.M., Wimmer, G., 2017. A new process for production of cement clinker from steelmaking slags. Cem. Int.

Xue, P., Xu, A., He, D., Yang, Q., Liu, G., Engström, F., Björkman, B., 2016. Research on the sintering process and characteristics of belite sulphoaluminate cement produced by BOF slag. Constr. Build. Mater. 122, 567–576. https://doi.org/10.1016/j.conbuildmat.2016.06.098.

Zhang, J., Ke, G., Liu, Y., 2021. Early hydration heat of calcium sulfoaluminate cement with influences of supplementary cementitious materials and water to binder ratio. Materials 14, 642. https://doi.org/10.3390/ma14030642.

Zhuang, S., Wang, Q., 2021. Inhibition mechanisms of steel slag on the early-age hydration of cement. Cem. Concr. Res. 140, 106283 https://doi.org/10.1016/j.cemconres.2020.106283.